Langmuir

Article

pubs.acs.org/Langmuir

Self-Assembly of Miktoarm Star-Like AB_n Block Copolymers: From Wet to Dry Brushes

Yuci Xu,*[†] Chao Wang,[†] Shuo Zhong,[†] Weihua Li,[‡] and Zhiqun Lin[§]

[†]Department of Polymer Science and Engineering, Faculty of Materials Science and Chemical Engineering, Key Laboratory of Specialty Polymers, Ningbo University, Ningbo, Zhejiang 315211, China

[‡]State Key Laboratory of Molecular Engineering of Polymer, Department of Macromolecular Science, Fudan University, Shanghai 200433, China

[§]School of Materials Science and Engineering, Georgia Institute of Technology, Atlanta, Georgia 30332, United States

Supporting Information

ABSTRACT: Self-assembly of miktoarm star-like AB_n block copolymer in both selective solvent (A- or B-selective) and miscible homopolymer matrix (A or B homopolymer), that is, formation of micelles, was for the first time investigated by theoretical calculations based on self-consistent mean field theory. Interestingly, the calculation revealed that the size of micelles in solvent was smaller than that in homopolymer under the same conditions. In B-selective solvent, with increasing number of B blocks n in miktoarm star-like AB_n block copolymer at a fixed volume fraction of A block, the micellar size decreased gradually. In stark contrast, when miktoarm star-like AB_n block copolymer dissolved in B homopolymer matrix at molecular weight ratio of B homopolymer to AB_n block copolymer $f_H = 0.30$, the overall micellar size decreased nonmonotonically as the number of B blocks n in AB_n block copolymer increased. The largest micelle was formed in AB_2 (i.e., $n = 2$). This intriguing finding can be attributed to a wet-to-dry brush transition that occurred from $n = 1$ to $n = 2$ in the micellization of miktoarm star-like AB_n block copolymer. Moreover, the micellization behaviors of miktoarm star-like AB_n block copolymer in A-selective solvent and A homopolymer matrix were also explored, where the overall micellar size in both scenarios was found to decrease monotonically as n in AB_n block copolymer increased. These self-assembled nanostructures composed of miktoarm star-like AB_n block copolymers may promise a wide range of applications in size-dependent drug delivery and bionanotechnology.

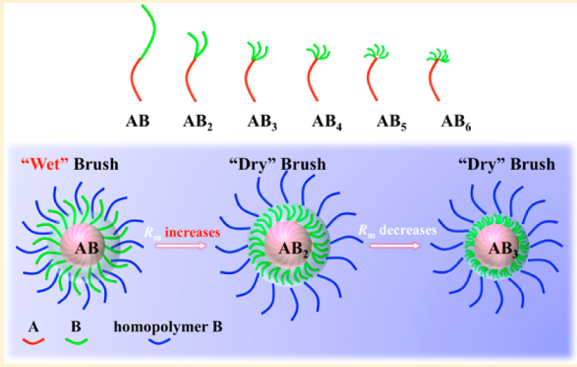

INTRODUCTION

Self-assembly of amphiphilic block copolymers in selective solvent has been the subject of intense research, as it provides a platform to form a myriad of aggregate structures of different size and shape,[1] including spherical micelles,[2−4] cylindrical or wormlike micelles, segmented micelles, bilayer vesicles, and helices.[5−7] Both fundamental understanding on self-assembly[8] and potential applications in cosmetics, drug delivery, and encapsulation technology[9−11] can be envisioned with these materials. Quite interestingly, upon mixing with the corresponding immiscible homopolymer mixtures, block copolymers often form micelles rather than simply situating at the interface between two immiscible homopolymers,[12,13] which has practical implications in polymer processing.[13,14]

In theory, for the formation of block copolymer micelles in selective solvent, the competition between interfacial energy at the interphase and conformational entropy of block copolymer dictates the equilibrium density profiles of micelle.[15,16] On the other hand, in the case of micellar formation in the mixture of block copolymer and homopolymer,[14] free energy of a single micelle composed of several block copolymer chains as well as homopolymer chains, translational entropy of micelles, and free energy of mixing homopolymer and the corona of block copolymer micelle all contribute to the total free energy and determine the micellar behavior. A set of equations can be yielded by minimization of total free energy, from which the fraction of copolymer chains aggregated into micelles can be computed, and the critical micelle concentration can thus be successfully obtained. Notably, self-consistent field theory (SCFT),[17−19] in particular spectral method,[20] real-space method,[21] and pseudospectral scheme of real-space method,[22,23] have been extensively employed to solve the modified diffusion equation (MDE) of the propagators, with which micellization of block copolymers in selective solvent as well as in homopolymer have been studied.[24−30] In addition to SCFT, the formation of such micelles was also intensively modeled by Monte Carlo (MC) simulations,[31−36] dynamical density

Received: January 9, 2015
Revised: February 15, 2015
Published: February 17, 2015

DOI: 10.1021/acs.langmuir.5b00081
Langmuir 2015, 31, 2905−2913

functional simulations (DFT), and dissipative particle dynamics (DPD).[37−39]

It is worth noting that micellization behavior for block copolymer (e.g., AB diblock copolymer) in selective solvent (either A- or B-selective) and in homopolymer matrix (e.g., either A or B homopolymer) is markedly different. In selective solvent, due to the larger entropy of small molecular solvent, the block polymer chains at the corona of the micelle tend to swell. These swollen micelles are called "wet" brushes.[40,41] In sharp contrast, in the case of homopolymer, the swelling behavior of block copolymer micelle depends heavily on the molecular weight of homopolymer. For short homopolymer (i.e., low molecular weight), the corona of block copolymer micelles is swollen and forms a wet brush. However, for homopolymer with higher molecular weight, it cannot effectively penetrate into the corona, thereby leading to the formation of "dry" brush. According to the wet and dry brush theory,[40,41] the molecular weight ratio of homopolymer, H, to miscible block, B, in block copolymer (for example, AB diblock copolymer, in which B block is miscible with homopolymer H), $\lambda = H/B$, differentiates the block copolymer micelle into dry-brush micelle ($\lambda \geq 1$) and wet-brush micelle ($\lambda < 1$). Obviously, the type of micelle exerts profound influence on the overall micelle size. However, the dependence of the type of micelles formed in selective solvent and in homopolymer matrix on micellization behavior has yet to be explored.

Herein, we report for the first time the self-assembly of miktoarm star-like AB_n block copolymer in selective solvent (either A- or B-selective) and homopolymer matrix (either A or B homopolymer) (i.e., forming micelles) by theoretical modeling. Miktoarm star-like AB_n block copolymers[42] carry many intriguing characteristics (e.g., hierarchical self-assembly[43,44] and adjustable degradation[45]), making them promising candidates for a wide range of potential applications in biomedical engineering, drug delivery, and nanotechnology.[46,47] The pseudospectral method of SCFT was employed to calculate overall micellar size R_m, micellar core radius R_c, and micellar corona thickness L_c. The micellar size of AB_n block copolymer (i.e., $n = 1$) in B-selective solvent was found to be smaller than that of the AB_n/B mixture (i.e., AB_n mixed with B homopolymer). In B-selective solvent, as the number of B blocks n in miktoarm star-like AB_n block copolymer increased with fixed volume fraction of A block, the overall micellar size decreased gradually (i.e., no wet-to-dry brush transition). Surprisingly, when AB_n block copolymer was dissolved in B homopolymer matrix at the molecular weight ratio of B homopolymer to AB_n block copolymer $f_H = 0.30$, the size of micelles decreased nonmonotonically with increasing n, where the largest micelle was yielded at $n = 2$ (i.e., from AB_2 block copolymer). Such an intriguing finding can be ascribed to the wet-to-dry brush transition occurring from $n = 1$ to $n = 2$ during the micellization of miktoarm star-like AB_n block copolymer. As the type of brush (i.e., either dry or wet brush) has great impact on the crystallization behavior[48] and the molecular exchange kinetics of block copolymer micelles,[49−51] it is of importance to scrutinize the micellization of AB_n block copolymer. Finally, the micellization behaviors of AB_n block copolymer in A-selective solvent and A homopolymer matrix were also explored, where the overall micellar size decreased gently in both cases as n increased.

THEORY

In this work, a binary blend consisting of incompressible melts of miktoarm star-like AB_n block copolymer in the presence of B-selective solvent (S) is first considered, where n is the number of B arms (i.e., blocks) in AB_n block copolymer. Each miktoarm star-like block copolymer has the same degree of polymerization N, and the degree of each B block is N_B/n, where N_B is the degree of polymerization of B block. The volume fractions of A and B blocks, f_A and f_B, are defined as N_A/N and N_B/N, respectively, where N_A is the degree of polymerization of A block in miktoarm star-like AB_n block copolymer. We define ϕ as the volume fraction of block copolymer. The interactions between i and j (i, j = A, B, and S) are characterized by Flory−Huggins interaction parameter χ_{ij}. The lengths in SCFT are expressed in units of the radius of gyration of linear polymer,[52,53] $R_g = (Nb^2/6)^{1/2}$, where b is the Kuhn length. According to many-chain Edwards theory,[17,18,54,55] the free energy functional F per chain can be given by eq 1 for miktoarm star-like AB_n block copolymer in the presence of B-selective solvent:

$$\frac{F}{k_BT} = -\phi \ln\left(\frac{Q_C}{\phi}\right) - (1-\phi)N \ln\left(\frac{Q_S}{1-\phi}\right) + \frac{1}{V}\int d\mathbf{r}\,\{\chi_{AB}N\phi_A(\mathbf{r})\phi_B(\mathbf{r}) + \chi_{AS}N\phi_A(\mathbf{r})\phi_S(\mathbf{r}) + \chi_{BS}N\phi_B(\mathbf{r})\phi_S(\mathbf{r}) - \omega_A(\mathbf{r})\phi_A(\mathbf{r}) - \omega_B(\mathbf{r})\phi_B(\mathbf{r}) - \omega_S(\mathbf{r})\phi_S(\mathbf{r}) - \eta(\mathbf{r})[1 - \phi_A(\mathbf{r}) - \phi_B(\mathbf{r}) - \phi_S(\mathbf{r})]\} \quad (1)$$

where $\phi_A(\mathbf{r})$and $\phi_B(\mathbf{r})$ are the monomer densities of A and B, respectively. Q_C and Q_S are the partition functions of a single block copolymer and a solvent molecule, respectively, given by eqs 2 and 3:

$$Q_C = \frac{1}{V}\int d\mathbf{r}\, q_K(\mathbf{r}, s)q_K^{\dagger}(\mathbf{r}, s) \quad (2)$$

$$Q_S = \frac{1}{V}\int d\mathbf{r}\, \exp\left[\frac{-\omega_s(\mathbf{r})}{N}\right] \quad (3)$$

where $q_K(\mathbf{r}, s)$ and $q_K^{\dagger}(\mathbf{r}, s)$ (K = A, B) are end-segment distribution functions, which are proportional to the probability that a polymer segment of contour length s and with one free end has its other end located at $\mathbf{r}$. These distribution functions satisfy the modified diffusion equations:

$$\frac{\partial q_K(\mathbf{r}, s)}{\partial s} = \nabla^2 q_K(\mathbf{r}, s) - \omega_K(\mathbf{r})q_K(\mathbf{r}, s) \quad (4)$$

$$-\frac{\partial q_K^{\dagger}(\mathbf{r}, s)}{\partial s} = \nabla^2 q_K^{\dagger}(\mathbf{r}, s) - \omega_K(\mathbf{r})q_K^{\dagger}(\mathbf{r}, s) \quad (5)$$

The initial conditions for eqs 4 and 5 are $q_A(\mathbf{r}, 0) = 1$ and $q_B^{\dagger}(\mathbf{r}, 1) = 1$, respectively. Minimization of the total free energy with respect to monomer densities and mean fields leads to the following standard mean-field equations:

$$\omega_A(\mathbf{r}) = \chi_{AB}N\phi_B(\mathbf{r}) + \chi_{AS}N\phi_S(\mathbf{r}) + \eta(\mathbf{r}) \quad (6)$$

$$\omega_B(\mathbf{r}) = \chi_{AB}N\phi_A(\mathbf{r}) + \chi_{BS}N\phi_S(\mathbf{r}) + \eta(\mathbf{r}) \quad (7)$$

$$\omega_S(\mathbf{r}) = \chi_{AS}N\phi_A(\mathbf{r}) + \chi_{BS}N\phi_B(\mathbf{r}) + \eta(\mathbf{r}) \quad (8)$$

$$\phi_A(\mathbf{r}) + \phi_B(\mathbf{r}) + \phi_S(\mathbf{r}) = 1 \quad (9)$$

$$\phi_A(\mathbf{r}) = \frac{\phi}{Q}\int_{s\in A} ds\, q_A(\mathbf{r}, s)q_A^{\dagger}(\mathbf{r}, s) \quad (10)$$

$$\phi_B(\mathbf{r}) = \frac{\phi}{Q}\int_{s\in B} ds\, q_B(\mathbf{r}, s)q_B^{\dagger}(\mathbf{r}, s) \quad (11)$$

DOI: 10.1021/acs.langmuir.5b00081
Langmuir 2015, 31, 2905−2913

$$\phi_S(\mathbf{r}) = \frac{1-\phi}{Q}\exp\left[\frac{-\omega_s(\mathbf{r})}{N}\right] \quad (12)$$

The split-step Fourier method[22,23] is employed to solve the modified diffusion equations for the end-segment distribution functions. Periodic boundary conditions are imposed automatically on the square cell in the split-step Fourier method. The box size chosen is $50 \times 50R_g$ and it is discretized into $N_x \times N_y = 256 \times 256$ lattices. We use various initial conditions to generate many micelles, and the micellar core, micellar corona, and overall micellar size are then calculated.

The SCFT equation in the presence of B homopolymer is similar to the equation described above. Thus, we avoid repetition of this equation. We note that $f_H N$ is used to describe the degree of polymerization of homopolymer, where f_H is the molecular weight ratio of B homopolymer to AB_n block copolymer as previously noted.

RESULTS AND DISCUSSION

Micellar Sizes as a Function of Number of Arms *n* in Miktoarm Star-like AB_n Block Copolymer in B-Selective Solvent and in B Homopolymer Matrix. To investigate the micellization behavior of miktoarm star-like AB_n block copolymer in B-selective solvent, we chose volume fractions of A and B in AB_n as $f_A = 0.40$ and $f_B = 0.60$, and the block copolymer concentration $\phi = 0.20$. The volume fraction of each B arm (Δf_B) is thus f_B/n. For n = 1, 2, 3, 4, 5, and 6, Δf_B is 0.60, 0.30, 0.20, 0.15, 0.12, and 0.10, respectively. The block copolymer chain contour length was divided into 100 points, and the discretization of box size is $N_x \times N_y = 256 \times 256$, which is sufficient to give reasonable results[24,56] (see the discretization test in Figure S1, Supporting Information). To ensure the formation of micelles, three Flory–Huggins interaction parameters $\chi_{AB}N$, $\chi_{AS}N$, and $\chi_{BS}N$ were chosen as 30, 50, and 10, respectively. Density plots of micelles are shown in Figure 1.

Boundaries between micelle core, micelle corona, and homopolymer B were not perfectly distinct in the calculation. We define the micellar core radius, R_c, as the value at which densities of the A and B blocks in AB_n block copolymer are equal: $\phi_A(\mathbf{r}) = \phi_B(\mathbf{r})$. Interestingly, the corona appeared to be rather diffusive, especially for AB_n in B-selective solvent (Figure 1a). Thus, the full width at half-maximum (fwhm) was used as a measure for the corona thickness, L_c (Figure S2, Supporting Information). The overall size of micelle, R_m, is the sum of R_c and L_c. Notably, eight samples were simulated for each n to ensure the structures were reproducible, and at least 200 micelles were included in the calculation of average micellar size. The variation of R_c, L_c, and R_m as a function of n is shown in Figure 2a. Clearly, R_c, L_c, and R_m decreased as n increased. For L_c, the decrease was due to the decrease of Δf_B. Notably, a sharp decrease of L_c from n = 1 to n = 2 was found. This is not surprising as Δf_B in AB_2 block copolymer ($\Delta f_B = 0.30$) was half that of AB ($\Delta f_B = 0.60$) diblock copolymer. In addition, R_c decreased slightly with increasing n, where the volume fraction of A block was fixed at $f_A = 0.40$. This is due to the micellar corona becoming dense when n increased (Figure S3, Supporting Information), leading to the decrease of aggregated numbers of miktoarm star-like chains. For self-assembly of miktoarm star-like AB_n block copolymer in B-selective solvent, the entropy of small solvent molecule dominated and the solvent can easily penetrate into the micellar corona, resulting in increased effective volume fraction of B block. The larger volume fraction of B block favored the increase of spontaneous curvature.[57] Consequently, small micelles were formed, which agreed well with previous experimental study.[25]

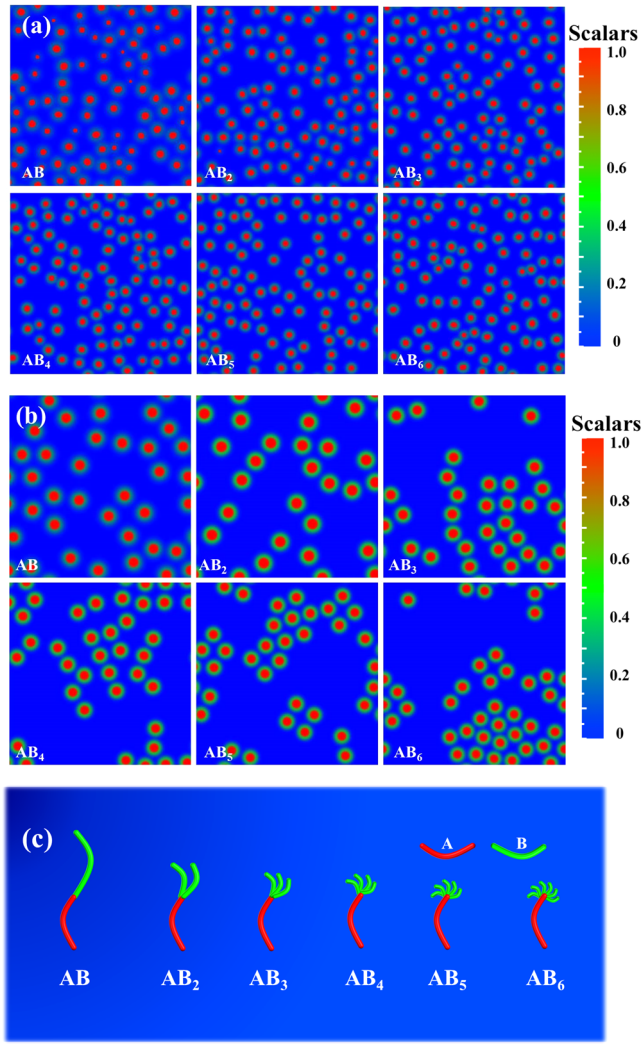

Figure 1. Formation of micelles of AB_n block copolymer in (a) B-selective solvent and (b) B homopolymer. Red, green, and blue represent the domains where the largest component is A in AB_n, B in AB_n, and B homopolymer, respectively. The parameters chosen in the calculation are as follows: (a) $f_A = 0.4$, $\phi = 0.20$, $\chi_{AB}N = 30$, $\chi_{AS}N = 50$, $\chi_{BS}N = 10$, and $L_x = L_y = 50R_g$. (b) $f_A = 0.4$, $\phi = 0.20$, $\chi_{AB}N = 30$, $f_H = 0.30$, and $L_x = L_y = 50$. (c) Schematic of AB_n miktoarm star-like block copolymers.

For a mixture containing AB_n block copolymer and B homopolymer, f_H was used to define the chain length of B homopolymer, as discussed above, and fixed at 0.30 to ensure the formation of isolated micelles, as the longer homopolymer chain caused the aggregation of micelles as shown in Figure S4 (Supporting Information). The Flory–Huggins interaction parameter between A and B blocks was selected to be the same as that in the case of AB_n block copolymer in B-selective solvent. We note that by deliberately adjusting the length of B block in AB_n block copolymer that is miscible with B homopolymer at the fixed molecular weight of B homopolymer, that is, by tuning f_H, the micellization behavior of AB_n block copolymer in the homopolymer matrix can be elaborated. Strikingly, the overall micellar size R_m was found to decrease nonmonotonically as n increased (Figure 2b). A maximum of R_m was seen at n = 2, and with a further increase in n, R_m decreased. In order to understand this interesting observation, micellar core radius R_c and micellar corona thickness L_c were

DOI: 10.1021/acs.langmuir.5b00081
Langmuir 2015, 31, 2905–2913

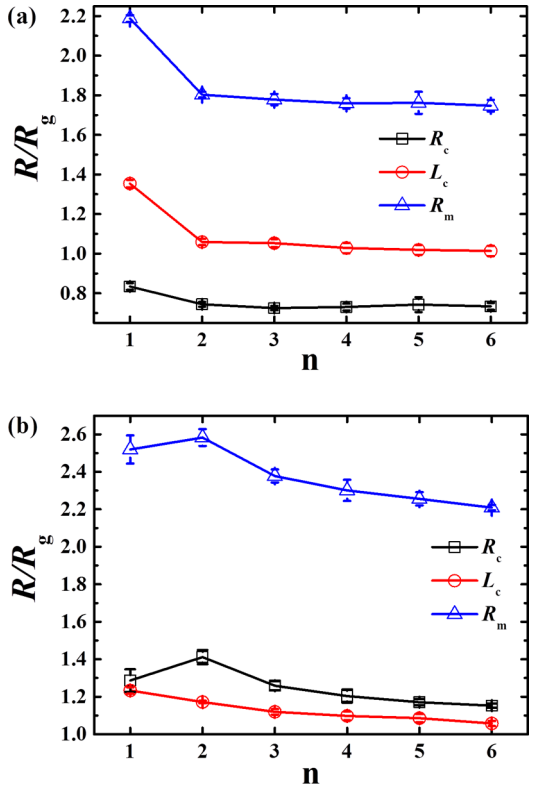

Figure 2. Calculated core radius, corona thickness, and overall micellar size of AB_n block copolymer in (a) B-selective solvent and (b) B homopolymer matrix as a function of the number of B arms n in AB_n block copolymer (lines are for guidance). Parameters chosen in the calculations are as follows: (a) $f_A = 0.4$, $\phi = 0.20$, $\chi_{AB}N = 30$, $\chi_{AS}N = 50$, and $\chi_{BS}N = 10$. (b) $f_A = 0.4$, $\phi = 0.20$, $\chi_{AB}N = 30$, and $f_H = 0.30$.

also calculated (Figure 2b). The plot of R_c showed that the AB_2 block copolymer had the largest core radius, which is consistent with that seen in R_m. However, L_c decreased gradually with increasing n. This can be attributed to the decrease of Δf_B, which is in good accordance with the results in selective solvent as discussed above (red circles in Figure 2a). As noted above, the ratio of molecular weight of homopolymer to that of miscible block B in the block copolymer, $\lambda = H/B$, governs the interfacial behavior of block copolymer micelles[13,40,41] (dry-brush micelle forms at $\lambda \geq 1$, and wet-brush micelle results at $\lambda < 1$). For $n = 1$, λ is 0.50. Thus, the B blocks on the micellar corona are expected to be wet (Figure S3d, Supporting Information). Penetration of B homopolymer into the micelle corona led to the increases volume fraction of B block, and a small micellar size was thus achieved (Figure 3). On the other hand, when n increased to 2, λ became 1.0. With the decrease of

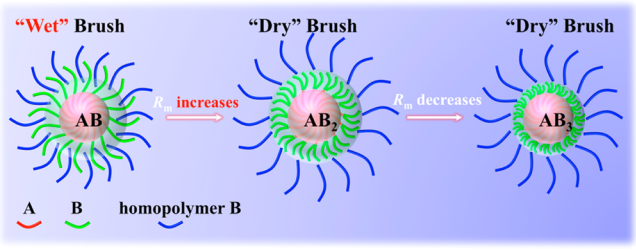

Figure 3. Schematic illustration of formation of the largest micelle of AB_n block copolymer at $n = 2$ in B homopolymer matrix at $f_H = 0.30$.

Δf_B, the penetrability of B homopolymer into the corona weakened; instead of penetrating into the corona, the homopolymer is expected to form an isolated region because of the high conformation entropy penalty. As a result, the homopolymer can no longer efficiently swell the block copolymer micelle, and a dry brush was thus formed that possessed an increased micellar size (Figure 3).[57] However, with further increase in n, the micellar corona became dense, which caused an increase of spontaneous curvature, thereby leading to the decrease of the micellar core radius (Figure 3). Taken together, during the wet-to-dry brush transition, this intriguing nonmonotonic micellization behavior emerged.

Influence of Molecular Weight of Homopolymer on Micellization. Subsequently, we explored the effect of molecular weight of B homopolymer f_H (i.e., molecular weight ratio of B homopolymer to AB_n block copolymer) on the micellization behavior of miktoarm star-like AB_n block copolymer in the B homopolymer matrix. Similarly, the dependence of R_c, L_c, and R_m on n at $f_H = 0.30$, 0.50, 0.60, and 0.65, respectively, were computed (Figure 4). For

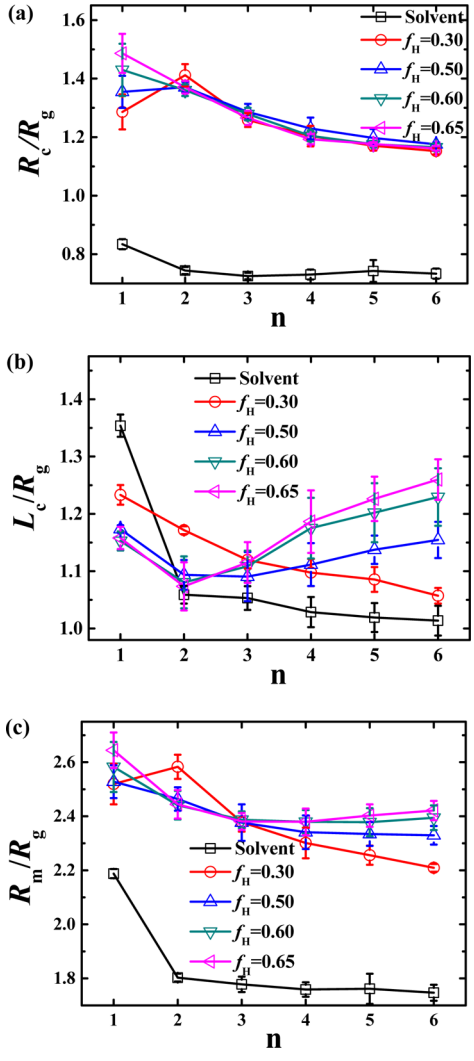

Figure 4. Calculated (a) micellar core radius, (b) micellar corona thickness, and (c) overall micellar size as a function of n at $f_H = 0.30$, 0.50, 0.60, and 0.65 for self-assembly of miktoarm star-like AB_n block copolymer in B homopolymer matrix and in B-selective solvent. We note that nonmonotonic behavior disappeared as f_H increased.

DOI: 10.1021/acs.langmuir.5b00081
Langmuir 2015, 31, 2905−2913

comparison, R_c, L_c, and R_m in B-selective solvent were also included in Figure 4. Because of the entropy effect of small solvent molecules, the micellar core radius R_c in selective solvent was the smallest (Figure 4a). As f_H increased but was smaller than 0.60, a maximum of R_c at $n = 2$ in AB_n occurred. When f_H was larger than 0.60, R_c decreased monotonically with increasing n. This micellization behavior can be rationalized by the fact that AB_n block copolymers in B homopolymer matrix formed the dry brush for all n: there was no wet-to-dry brush transition as n increased, and thus the micellar core radius R_c of AB diblock copolymer (i.e., n =1) was the largest (Figure 4a). As f_H increased, R_c increased slightly for each fixed n, which is consistent with the prediction of LOW-Roe theory.[14,58,59]

The effect of f_H on micellar corona thickness L_c as a function of n is depicted in Figure 4b. For AB_n block copolymer in B-selective solvent, as the corona was strongly swollen by solvent, AB diblock copolymer (i.e., $n = 1$) had the largest L_c. Notably, for the AB_n/B mixture, Δf_B had great influence on L_c. When f_H was small (i.e., $f_H = 0.30$), L_c decreased gradually as n increased. However, for the longer homopolymer (i.e., larger f_H), L_c decreased first and then increased as n increased. The decrease of L_c resulted from the decrease of Δf_B. On the other hand, larger n led to stretching of the corona block (i.e., B block) as the chains in the micellar corona were denser, causing the increase of L_c. The delicate balance between these two competing factors resulted in the nonmonotonic behavior of L_c. Larger L_c was obtained with the further increase in f_H, which can be attributed to the increase of $\lambda = H/B$ ratio (as described above) when f_H increased, thereby giving rise to increased corona thickness.

Figure 4c compares the influence of f_H on overall micellar size R_m. Obviously, the micelle formed in B-selective solvent had the smallest size due to the entropy effect of solvent. For the AB_n/B mixture, however, overall micellar size increased as f_H increased. It is worth noting that the nonmonotonic behavior of micellar size diminished at $f_H = 0.65$, where all AB_n block copolymers produced wet-brush micelles according to the above-mentioned dry and wet brush theory.[40,41] When f_H was larger than 0.50, the overall micellar size R_m decreased gradually as n increased. However, when $\lambda = H/B < 1.0$, wet brush was formed at $n = 1$, leading to the nonmonotonic behavior of R_m as a function of n.

Maximum Corona Density of Micelle in the Mixture of AB_n Block Copolymer and B Homopolymer. To measure the interfacial activity of micellar corona, the maximum corona density (MCD) (Figure S2, Supporting Information) of micelle was calculated (Figure 5), which would otherwise be difficult to observe experimentally. Especially, the definition of MCD is very useful for micellar drug delivery systems, where the delivery of drug can be controlled by tuning the corona density. The f_H values chosen in the calculations were 0.30, 0.50, 0.60, and 0.65. The curve with black squares described the MCD of AB_n block copolymer in B-selective solvent. As wet brush was yielded for all n, where the corona was strongly swollen by solvent, the MCD was lower than that formed in the B homopolymer case. The increase of MCD as n increased can be ascribed to the increase of n at the corona.

For the AB_n/B mixture, the MCD differed largely from that formed in B-selective solvent. From $n = 1$ to $n = 2$, there was a sharp increase of MCD at fixed f_H, signifying the transition from wet brush to try brush. Clearly, when $n > 2$, dry brushes were formed. Consequently, the MCD did not change appreciably (only slightly increased) as n increased. The

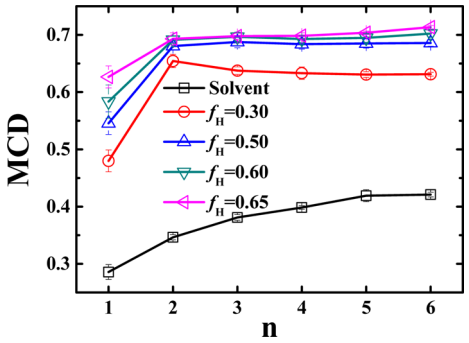

Figure 5. Maximum corona density (MCD) as a function of n for self-assembly of miktoarm star-like AB_n block copolymer in B-selective solvent and B homopolymer matrix at $f_H = 0.30$, 0.50, 0.60, and 0.65. The sharp increase of MCD signifies the wet-to-dry brush transition.

MCD increased with increasing f_H. The penetrability of homopolymer decreased with increasing f_H, leading to the decrease of MCD.

Influence of χN on Micellization Behavior. It is well-known that the χ parameter determines the domain size in self-assembly of block copolymers.[20,60] Thus, the influence of χ parameter on the micellization behavior of AB_n block copolymer in B homopolymer matrix was investigated. The corresponding R_c, L_c, R_m, and MCD were computed and are summarized in Figure 6. In the calculations, χN values of 30, 31, 32, 33, 34, and 35 were chosen. As χN increased, R_c, L_c, and R_m showed a trend of decrease. This is because of chain stretching due to increasing χN, thereby leading to the penetration of homopolymer into the micellar corona (Figure 7). Consequently, wet brush was formed. In comparison to the maximum micellar size found at $n = 2$ for $\chi N = 30$, the maximum size of micelle occurred at $n = 3$ for $\chi N = 32$, indicating the wet-to-dry brush transition shifted toward larger n. With a further increase of χN to 33, the maximum size emerged in the AB_4 block copolymer. This shift was clearly manifested in the MCD plot shown in Figure 6d. As χN increased, MCD, reflecting the penetration of homopolymer into corona, decreased.

On the basis of the above results, it is clear that larger χN led to the formation of smaller micelles. Moreover, as χN increased, the wet-to-dry brush transition moved toward larger n.

AB_n Block Copolymer in A-Selective Solvent and A Homopolymer. We now turn our attention to explore the micellization behavior of miktoarm star-like AB_n block copolymer in A-selective solvent and A homopolymer matrix. In these two cases, the B blocks formed the core of the micelle with A blocks as the corona. As n increased, $\lambda = H/B$ was constant as A blocks, which were located at the corona, became the miscible block. Likewise, in order to gain a systematic understanding of the self-assembly of miktoarm star-like AB_n block copolymer in A-selective solvent and A homopolymer matrix, R_c, L_c, and R_m as a function of n were calculated (Figure 8). The Flory–Huggins parameters were chosen to be $\chi_{AB}N = 30$, $\chi_{AS}N = 10$ and $\chi_{BS}N = 50$, which are identical to those in B-selective solvent. The volume fraction of A block, f_A, was 0.40. Figure 8a shows that overall micellar size R_m and micellar core radius R_c decreased as n increased, while micellar corona L_c tended to increase as a function of n. Notably, compared with the sharp decrease of micellar size R_m from $n = 1$ (i.e., AB) to $n = 2$ (i.e., AB_2) in B-selective solvent (Figure 2a), only a slight decrease of micellar size R_m occurred in A-selective solvent

DOI: 10.1021/acs.langmuir.5b00081
Langmuir 2015, 31, 2905−2913

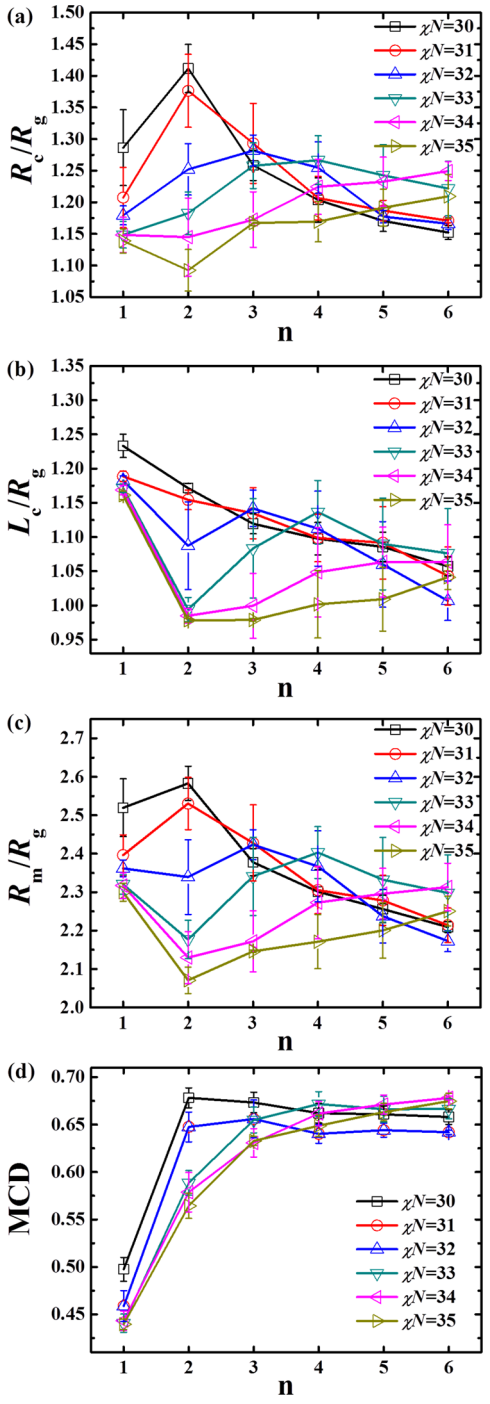

Figure 6. Influence of χN on (a) micellar core radius, (b) micellar corona thickness, (c) overall micellar size, and (d) corresponding MCD at f_H = 0.30 for self-assembly of miktoarm star-like AB_n block copolymer in B homopolymer. The wet-to-dry brush transition shifted toward larger n as χN increased.

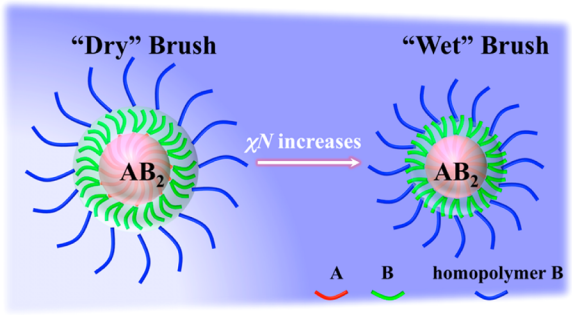

Figure 7. Schematic illustration of influence of χN on micellar size for self-assembly of miktoarm star-like AB_n block copolymer in B homopolymer matrix at f_H = 0.30. The increase of χN induced stretching of AB_n block copolymer, thus leading to penetration of homopolymer into the micellar corona. As a result, the micellar size decreased.

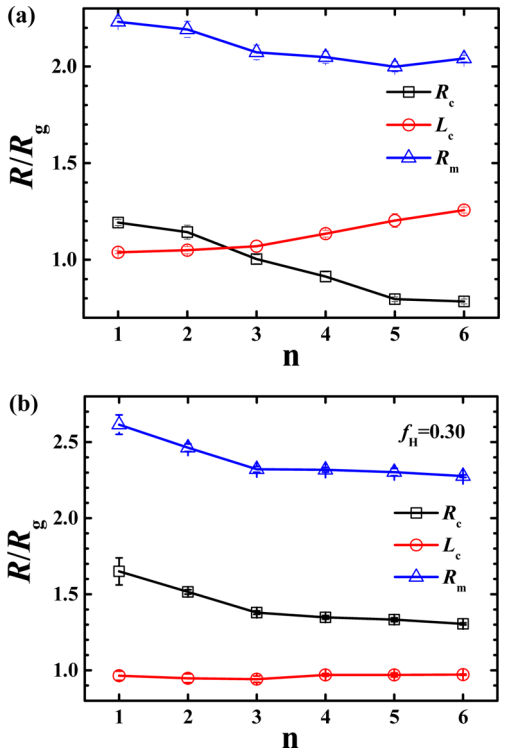

Figure 8. R_c, L_c, and R_m as a function of n for self-assembly of miktoarm star-like AB_n block copolymer in (a) A-selective solvent and (b) A homopolymer matrix at f_H = 0.30.

(Figure 8a). From Figures 2a and 8a, it is clear that the micellar size of n = 2 (i.e., AB_2) in A-selective solvent is larger than that in B-selective solvent, as the branch block constituted the core in A-selective solvent (Figure S6, Supporting Information). This is in good agreement with the experimental results where the micellar size of $(PI)_2PS$ (I_2S), $(PS)_2PI$ (S_2I), and PSPI (SI) diblock copolymer in n-decane (selective solvent for polyisoprene, PI) was found to decrease in the order SI > S_2I > I_2S.[25] The explanation of this tendency was clearly demonstrated in Figure S6 (Supporting Information). The decrease of R_c resulted from the decrease of Δf_B (i.e., B block, that is, core block). The increase of L_c can be attributed to the low graft density of A block (i.e., corona block) on the core as n increased, thus leading to diffusion of A block.

On the other hand, when miktoarm star-like AB_n block copolymers self-assembled in A homopolymer at f_H = 0.30 (density plots are shown in Figure S5, Supporting Information), the micellization behaviors differed from those in Figure 2b, as clearly evidenced in Figure 8b, where R_c and R_m decreased monotonically as n increased due to the decrease of Δf_B (core block). It is interesting to note that L_c remained almost the same as n increased, which is not surprising as $\lambda = H/B$ was independent of n when the micellar corona was composed of A blocks. Intriguingly, nonspherical micelles, such

DOI: 10.1021/acs.langmuir.5b00081
Langmuir 2015, 31, 2905−2913

as wormlike micelles, were found in A-selective solvent and A homopolymer matrix (Figure S5, Supporting Information). The formation of wormlike micelles was a direct consequence of the increasing volume fraction of core block (i.e. B block), which correlated well with the experimental observation on wormlike micelles self-assembled from miktoarm star-like poly(γ-benzyl-L-glutamate)/linear poly(ethylene oxide) block copolymer (i.e., AB_n type D_m-PBLG-*b*-PEO) in aqueous solution when the volume fraction of core block, f_{PBLG}, increased.[45]

For self-assembly of miktoarm star-like AB_n block copolymer in A-selective solvent and A homopolymer, the dependence of micellization behavior on f_H is expected to be largely different from that in B-selective solvent and B homopolymer discussed above, due to the packing frustration where the branched B blocks constituted the micellar core (Figure S7, Supporting Information). For the micellization of miktoarm star-like AB_n block copolymer in A homopolymer, R_c, L_c, R_m, and MCD as a function of n at different f_H were calculated (Figure 9). For all f_H values, R_c and R_m decreased gradually as n increased. As there were no dry-to-wet brush transitions, the nonmonotonic behavior was not identified in A homopolymer for all f_H. Two pieces of information, that is, R_c increased as f_H increased and R_m in A-selective solvent had the smallest radius, were in good agreement with the results in Figure 4. The dependence of L_c on f_H was rather complex (Figure 9b). For miktoarm star-like AB_n block copolymer in the A-selective solvent, the micellar corona was the thickest due to strongly swollen corona block in solvent. When the micelle was formed in A homopolymer, L_c decreased with increasing f_H. The corona thickness depended heavily on the swelling degree of corona. The longer homopolymer chain led to compression of the corona block and thus a decrease of L_c. The degree of swelling can be readily represented by maximum corona density (Figure 9d). With increasing n, L_c at different f_H values tended to increase. Figure 9c describes the influence of f_H on R_m. For f_H = 0.30, the wet brush was formed. Accordingly, a small micellar size resulted. As f_H increased, the degree of dry brush increased, and thus the larger R_m was achieved.

In order to evaluate the degree of dry brush, calculations on the MCD of miktoarm star-like AB_n block copolymer in A-selective solvent and A homopolymer as a function of n at different f_H values were performed (Figure 9d). Obviously, as the B blocks constituted the micellar core, the MCD differed completely from that in Figure 5. It is interesting to note that there was no sharp variation of MCD for AB_n block copolymer in A homopolymer, suggesting no wet-to-dry brush transition of micelles under this condition. In particular, the MCD decreased as n increased. Such decrease of MCD was due to the fact that low graft density of A block was achieved, and thus the micellar corona became diffusive. Moreover, MCD increased as f_H increased, which is consistent with the findings in Figure 5.

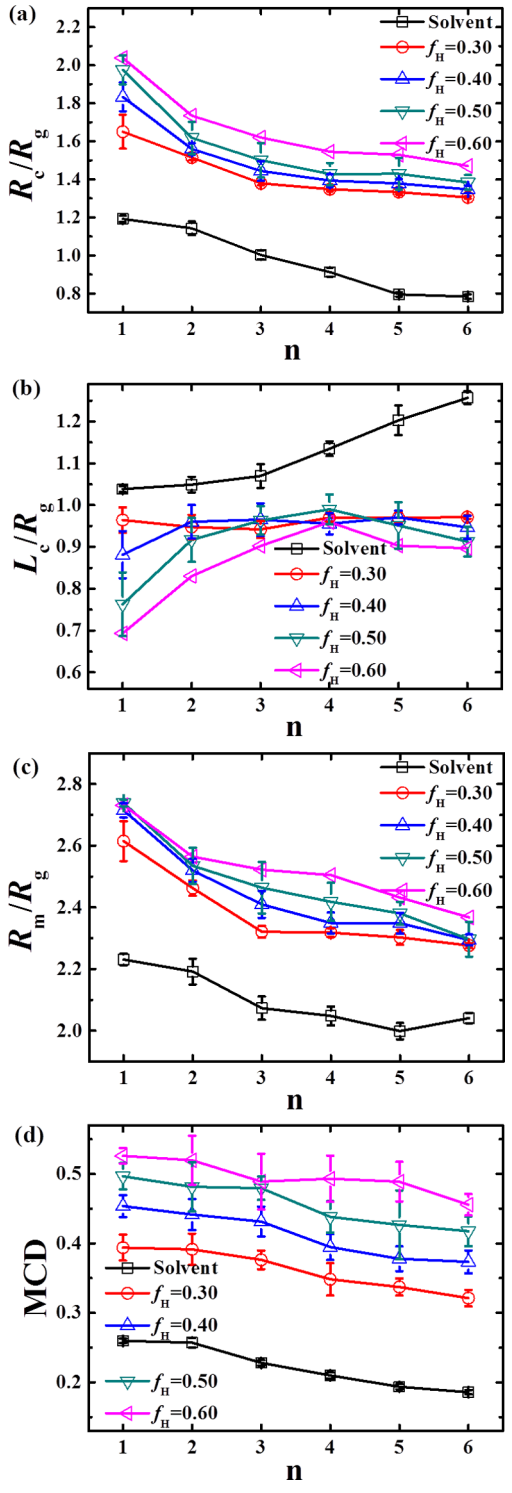

Figure 9. Influence of A homopolymer chain length on (a) micellar core radius, (b) micellar corona thickness, (c) overall micellar size, and (d) MCD for self-assembly of AB_n block copolymer in A-selective solvent and A homopolymer.

CONCLUSIONS

In summary, we systematically explored the self-assembly of miktoarm star-like AB_n block copolymer in A- and B-selective solvents as well as in A and B homopolymer matrices (i.e., formation of micelles) by self-consistent mean field theory calculations. Because of the larger entropy of small solvent molecules, overall micellar size in B-selective solvent was smaller than that in B homopolymer under the same conditions. With increasing number of B blocks n at fixed volume fraction of A block in B-selective solvent, the overall micellar size decreased monotonically. Quite intriguingly, when AB_n block copolymer dissolved in B homopolymer at f_H = 0.30, the overall micellar size was found to decrease nonmonotonically, and the micelle formed from AB_2 possessed the largest size. This can be ascribed to a wet-to-dry brush transition occurred from n = 1 to n = 2. With further increase of f_H, such a transition disappeared as dry brushes formed for all miktoarm star-like AB_n block copolymers (n = 1−6). In addition, the

DOI: 10.1021/acs.langmuir.5b00081
Langmuir 2015, 31, 2905−2913

maximum corona density MCD at different f_H values, signifying the degree of swelling of the micellar corona, was calculated. Finally, micellization behaviors of miktoarm star-like AB_n block copolymer in A-selective solvent and A homopolymer were also scrutinized. A monotonic decrease in micellar size prevailed in A-selective solvent and A homopolymer as n increased. Our calculations provided a fundamental understanding of wet and dry brushes of micelles composed of miktoarm star-like AB_n block copolymers. These self-assembled nanostructures may hold promise for applications in size-dependent nanocarriers, delivery vehicles, encapsulation technology, and bionanotechnology.

■ ASSOCIATED CONTENT

Supporting Information

Seven figures showing micellar size as a function of n in AB_n block copolymer at different discretizations; definition of micellar core radius R_c, micellar corona thickness L_c, and maximum corona density MCD; representative micelles in B-selective solvent and B homopolymer; density plots of micelles formed in AB_6 and B homopolymer; formation of micelles in A-selective solvent and A homopolymer; and schematics of micelle formation in A- and B-selective solvents and in A homopolymer. This material is available free of charge via the Internet at http://pubs.acs.org.

■ AUTHOR INFORMATION

Corresponding Author

*E-mail xuyuci@nbu.edu.cn (Y.X.).

Notes

The authors declare no competing financial interest.

■ ACKNOWLEDGMENTS

This work was supported by the National Natural Science Foundation of China (Grants 21304051 and 21322407), Zhejiang Xinmiao Program (Grants 2014R405090) (C.W.), and the Air Force Office of Scientific Research (FA9550-13-1-0101) (Z.L.). Y.C. gratefully acknowledges the support from K. C. Wong Magna Foundation at Ningbo University. We thank Rong Wang for useful discussion.

■ REFERENCES

(1) Zhang, L. F.; Eisenberg, A. Multiple Morphologies of Crew-Cut Aggregates of Polystyrene-*b*-Poly(acrylic acid) Block-Copolymers. *Science* **1995**, *268*, 1728−1731.

(2) Pang, X.; Zhao, L.; Akinc, M.; Kim, J. K.; Lin, Z. Novel Amphiphilic Multi-Arm, Star-Like Block Copolymers as Unimolecular Micelles. *Macromolecules* **2011**, *44*, 3746−3752.

(3) Pang, X.; Zhao, L.; Feng, C.; Lin, Z. Novel Amphiphilic Multiarm, Star-like Coil-Rod Diblock Copolymers via a Combination of Click Chemistry with Living Polymerization. *Macromolecules* **2011**, *44*, 7176−7183.

(4) Pang, X.; Zhao, L.; Han, W.; Xin, X.; Lin, Z. A General and Robust Strategy for the Synthesis of Nearly Monodisperse Colloidal Nanocrystals. *Nat. Nanotechnol.* **2013**, *8*, 426−431.

(5) Bailey, T. S.; Pham, H. D.; Bates, F. S. Morphological Behavior Bridging the Symmetric AB and ABC States in the Poly(styrene-*b*-isoprene-*b*-ethylene oxide) Triblock Copolymer System. *Macromolecules* **2001**, *34*, 6994−7008.

(6) Schlaad, H.; Kukula, H.; Smarsly, B.; Antonietti, M.; Pakula, T. Solid-State Morphologies of Linear and Bottlebrush-Shaped Polystyrene-Poly(Z-L-lysine) Block Copolymers. *Polymer* **2002**, *43*, 5321−5328.

(7) Hayward, R. C.; Pochan, D. J. Tailored Assemblies of Block Copolymers in Solution: It Is All about the Process. *Macromolecules* **2010**, *43*, 3577−3584.

(8) Zhulina, E. B.; Adam, M.; LaRue, I.; Sheiko, S. S.; Rubinstein, M. Diblock Copolymer Micelles in a Dilute Solution. *Macromolecules* **2005**, *38*, 5330−5351.

(9) Discher, D. E.; Eisenberg, A. Polymer Vesicles. *Science* **2002**, *297*, 967−973.

(10) Zhang, L. F.; Yu, K.; Eisenberg, A. Ion-Induced Morphological Changes in "Crew-Cut" Aggregates of Amphiphilic Block Copolymers. *Science* **1996**, *272*, 1777−1779.

(11) Li, X. A.; Tang, P.; Qiu, F.; Zhang, H. D.; Yang, Y. L. Aggregates in Solution of Binary Mixtures of Amphiphilic Diblock Copolymers with Different Chain Length. *J. Phys. Chem. B* **2006**, *110*, 2024−2030.

(12) Sundararaj, U.; Macosko, C. W. Drop Breakup and Coalescence in Polymer Blends: The Effects of Concentration and Compatibilization. *Macromolecules* **1995**, *28*, 2647−2657.

(13) Adedeji, A.; Lyu, S.; Macosko, C. W. Block Copolymers in Homopolymer Blends: Interface vs Micelles. *Macromolecules* **2001**, *34*, 8663−8668.

(14) Leibler, L.; Orland, H.; Wheeler, J. C. Theory of Critical Micelle Concentration for Solutions of Block Copolymers. *J. Chem. Phys.* **1983**, *79*, 3550−3557.

(15) Noolandi, J.; Hong, K. M. Interfacial Properties of Immiscible Homopolymer Blends in the Presence of Block Copolymers. *Macromolecules* **1982**, *15*, 482−492.

(16) Noolandi, J.; Hong, K. M. Theory of Block Copolymer Micelles in Solution. *Macromolecules* **1983**, *16*, 1443−1448.

(17) Edwards, S. F. Statistical Mechanics of Polymers with Excluded Volume. *Proc. Phys. Soc. London* **1965**, *85*, 613−624.

(18) Helfand, E. Theory of Inhomogeneous Polymers: Fundamentals of Gaussian Random-Walk Model. *J. Chem. Phys.* **1975**, *62*, 999−1005.

(19) Leibler, L. Theory of Microphase Separation in Block Copolymers. *Macromolecules* **1980**, *13*, 1602−1617.

(20) Matsen, M. W.; Schick, M. Stable and Unstable Phases of a Diblock Copolymer Melt. *Phys. Rev. Lett.* **1994**, *72*, 2660−2663.

(21) Drolet, F.; Fredrickson, G. H. Combinatorial Screening of Complex Block Copolymer Assembly with Self-Consistent Field Theory. *Phys. Rev. Lett.* **1999**, *83*, 4317−4320.

(22) Rasmussen, K. O.; Kalosakas, G. Improved Numerical Algorithm for Exploring Block Copolymer Mesophases. *J. Polym. Sci., Part B: Polym. Phys.* **2002**, *40*, 1777−1783.

(23) Tzeremes, G.; Rasmussen, K. O.; Lookman, T.; Saxena, A. Efficient Computation of the Structural Phase Behavior of Block Copolymers. *Phys. Rev. E* **2002**, *65*, No. 041806.

(24) Wang, R.; Tang, P.; Qiu, F.; Yang, Y. L. Aggregate Morphologies of Amphiphilic ABC Triblock Copolymer in Dilute Solution Using Self-Consistent Field Theory. *J. Phys. Chem. B* **2005**, *109*, 17120−17127.

(25) Pispas, S.; Hadjichristidis, N.; Potemkin, I.; Khokhlov, A. Effect of Architecture on the Micellization Properties of Block Copolymers: A_2B Miktoarm Stars vs AB Diblocks. *Macromolecules* **2000**, *33*, 1741−1746.

(26) Wang, J. F.; Guo, K. K.; An, L. J.; Muller, M.; Wang, Z. G. Micelles of Coil-Comb Block Copolymers in Selective Solvents: Competition of Length Scales. *Macromolecules* **2010**, *43*, 2037−2041.

(27) Sandoval, R. W.; Williams, D. E.; Kim, J.; Roth, C. B.; Torkelson, J. M. Critical Micelle Concentrations of Block and Gradient Copolymers in Homopolymer: Effects of Sequence Distribution, Composition, and Molecular Weight. *J. Polym. Sci., Part B: Polym. Phys.* **2008**, *46*, 2672−2682.

(28) Gido, S. P.; Wang, Z. G. Interfacial Curvature in Graft and Diblock Copolymers and Implications for Long-Range Order in Cylindrical Morphologies. *Macromolecules* **1997**, *30*, 6771−6782.

(29) Ye, X.-G.; Sun, Z.-Y.; Li, H.-F.; An, L.-J.; Tong, Z. The Phase Behavior of Comblike Block Copolymer $A_{m+1}B_m$/Homopolymer A Mixtures. *J. Chem. Phys.* **2008**, *128*, No. 094903.

DOI: 10.1021/acs.langmuir.5b00081
Langmuir 2015, 31, 2905−2913

(30) Greenall, M. J.; Gompper, G. Simple and Complex Micelles in Amphiphilic Mixtures: A Coarse-Grained Mean-Field Study. *Macromolecules* **2012**, *45*, 525−535.
(31) Pepin, M. P.; Whitmore, M. D. Homopolymer Solubilization Limits in Copolymer Micelles: A Monte Carlo Study. *Macromolecules* **2000**, *33*, 8654−8662.
(32) Pepin, M. P.; Whitmore, M. D. Monte Carlo and Mean Field Study of Diblock Copolymer Micelles. *Macromolecules* **2000**, *33*, 8644−8653.
(33) He, X. H.; Liang, H. J.; Pan, C. Y. Monte Carlo Simulation of Morphologies of Self-Assembled Amphiphilic Diblock Copolymers in Solution. *Phys. Rev. E* **2001**, *63*, No. 031814.
(34) Liang, H. J. Compatibility of Triblock Copolymers in an A/B/ Copolymer Ternary Mixture. *Macromolecules* **1999**, *32*, 8204−8209.
(35) Liang, H. J.; He, X. H.; Jiang, W.; Jiang, B. Z. Monte Carlo Simulation of Phase Separation of A/B/A-B Ternary Mixtures. *Macromol. Theory Simul.* **1999**, *8*, 173−178.
(36) Kong, W. X.; Li, B. H.; Jin, Q. H.; Ding, D. T.; Shi, A. C. Complex Micelles from Self-Assembly of ABA Triblock Copolymers in B-Selective Solvents. *Langmuir* **2010**, *26*, 4226−4232.
(37) Zhao, Y.; You, L. Y.; Lu, Z. Y.; Sun, C. C. Dissipative Particle Dynamics Study on the Multicompartment Micelles Self-Assembled from the Mixture of Diblock Copolymer Poly(ethyl ethylene)-*block*-Poly(ethylene oxide) and Homopolymer Poly(propylene oxide) in Aqueous Solution. *Polymer* **2009**, *50*, 5333−5340.
(38) Hsu, Y. C.; Huang, C. I.; Li, W. H.; Qiu, F.; Shi, A. C. Micellization of Linear A-*b*-(B-*alt*-C)$_n$ Multiblock Terpolymers in A-Selective Solvents. *Polymer* **2013**, *54*, 431−439.
(39) Huang, C. I.; Liao, C. H.; Lodge, T. P. Multicompartment Micelles from A_2-*star*-(B-*alt*-C) Block Terpolymers in Selective Solvents. *Soft Matter* **2011**, *7*, 5638−5647.
(40) Leibler, L. Emulsifying Effects of Block Copolymers in Incompatible Polymer Blends. *Makromol. Chem. Macromol. Symp.* **1988**, *16*, 1−17.
(41) Leibler, L. Block Copolymers at Interfaces. *Physica A* **1991**, *172*, 258−268.
(42) Iatridi, Z.; Tsitsilianis, C. Water-Soluble Stimuli Responsive Star-Shaped Segmented Macromolecules. *Polymers* **2011**, *3*, 1911−1933.
(43) Xie, N.; Li, W.; Qiu, F.; Shi, A. C. Sigma Formed in Conformationally Asymmetric AB-Type Block Copolymers. *ACS Macro Lett.* **2014**, *3*, 906−910.
(44) Xie, N.; Liu, M.; Deng, H.; Li, W.; Qiu, F.; Shi, A. C. Macromolecular Metallurgy of Binary Mesocrystals via Designed Multiblock Terpolymers. *J. Am. Chem. Soc.* **2014**, *136*, 2974−2977.
(45) Peng, S. M.; Chen, Y.; Hua, C.; Dong, C. M. Dendron-like Polypeptide/Linear Poly(ethylene oxide) Biohybrids with both Asymmetrical and Symmetrical Topologies Synthesized via the Combination of Click Chemistry and Ring-Opening Polymerization. *Macromolecules* **2009**, *42*, 104−113.
(46) Lee, C. C.; MacKay, J. A.; Frechet, J. M. J.; Szoka, F. C. Designing Dendrimers for Biological Applications. *Nat. Biotechnol.* **2005**, *23*, 1517−1526.
(47) Svenson, S.; Tomalia, D. A. Commentary - Dendrimers in Biomedical Applications - Reflections on the Field. *Adv. Drug Delivery Rev.* **2005**, *57*, 2106−2129.
(48) Luo, C. Y.; Han, X.; Gao, Y.; Liu, H. L.; Hu, Y. Crystallization Behavior of "Wet Brush" and "Dry Brush" Blends of PS-*b*-PEO-*b*-PS/ h-PEO. *J. Appl. Polym. Sci.* **2009**, *113*, 907−915.
(49) Gohr, K.; Schartl, W. Dynamics of Copolymer Micelles in a Homopolymer Melt: Influence of the Matrix Molecular Weight. *Macromolecules* **2000**, *33*, 2129−2135.
(50) Lu, J.; Choi, S.; Bates, F. S.; Lodge, T. P. Molecular Exchange in Diblock Copolymer Micelles: Bimodal Distribution in Core-Block Molecular Weights. *ACS Macro Lett.* **2012**, *1*, 982−985.
(51) Choi, S. H.; Bates, F. S.; Lodge, T. P. Molecular Exchange in Ordered Diblock Copolymer Micelles. *Macromolecules* **2011**, *44*, 3594−3604.
(52) Xu, Y.; Li, W.; Qiu, F.; Yang, Y. Self-Assembly of ABC Star Triblock Copolymers under a Cylindrical Confinement. *J. Phys. Chem. B* **2009**, *113*, 11153−11159.
(53) Xu, Y.; Li, W.; Qiu, F.; Lin, Z. Self-Assembly of 21-Arm Star-Like Diblock Copolymer in Bulk and under Cylindrical Confinement. *Nanoscale* **2014**, *6*, 6844−6852.
(54) Fredrickson, G. H. *The Equilibrium Theory of Inhomogeneous Polymers*. Oxford University Press: Oxford, U.K., 2006.
(55) Shi, A.-C. Self-Consistent Field Theory of Block Copolymers. In *Development in Block Copolymer Science and Technology*; Hamley, I. W., Ed.; Wiley: New York, 2004; Chapt. 8, pp 265−293.
(56) Wang, R.; Jiang, Z. B.; Chen, Y. L.; Xue, G. Surface-Induced Phase Transition of Asymmetric Diblock Copolymer in Selective Solvents. *J. Phys. Chem. B* **2006**, *110*, 22726−22731.
(57) Larue, I.; Adam, M.; Zhulina, E. B.; Rubinstein, M.; Pitsikalis, M.; Hadjichristidis, N.; Ivanov, D. A.; Gearba, R. I.; Anokhin, D. V.; Sheiko, S. S. Effect of the Soluble Block Size on Spherical Diblock Copolymer Micelles. *Macromolecules* **2008**, *41*, 6555−6563.
(58) Roe, R. J. Small-Angle X-ray-Scattering Study of Micelle Formation in Mixtures of Butadiene Homopolymer and Styrene Butadiene Block Copolymer. 3. Comparison with Theory. *Macromolecules* **1986**, *19*, 728−731.
(59) Kinning, D. J.; Thomas, E. L.; Fetters, L. J. Morphological-Studies of Micelle Formation in Block Copolymer Homopolymer Blends: Comparison with Theory. *Macromolecules* **1991**, *24*, 3893−3900.
(60) Matsen, M. W. The Standard Gaussian Model for Block Copolymer Melts. *J. Phys.: Condens. Matter* **2002**, *14*, R21−R47.

DOI: 10.1021/acs.langmuir.5b00081
Langmuir 2015, 31, 2905−2913